J|A|C|S
COMMUNICATIONS

Published on Web 10/13/2006

A General Synthetic Strategy for Oxide-Supported Metal Nanoparticle Catalysts

Nanfeng Zheng and Galen D. Stucky*

Department of Chemistry and Biochemistry, University of California, Santa Barbara, California 93106

Received August 17, 2006; E-mail: stucky@chem.ucsb.edu

Gold nanoparticles, particularly with dimension less than 10 nm, exhibit unexpectedly high catalytic activities toward different types of reactions, a property not revealed in bulk gold.[1−4] In order to obtain high catalytic activity, gold nanoparticles are generally dispersed on support materials, among which oxides are commonly used.[5] The overall performance of a supported gold nanoparticle catalyst highly depends on the size and shape of the gold nanoparticles, the structure and properties of oxide supports, and the gold−oxide interface interactions.[5,6] Although several techniques have been developed to prepare oxide-supported gold nanoparticles, they do not allow precise control over these parameters. Consequently, some reported results on gold catalysis are controversial and even partly contradictory.[7,8] A new synthetic strategy is needed that makes it possible to tune each of the above factors for supported gold nanoparticles.

We have developed a general strategy to prepare oxide-supported metal nanoparticle catalysts, which is applicable to acidic and basic oxides. In addition to its versatility, the approach permits facile control over different parameters of a supported metal nanoparticle catalyst (e.g., particle size, size-distribution, loading). The effect of oxide supports in determining the size and size dispersion of gold nanoparticles is minimized because the gold nanoparticles are synthesized before they are immobilized on the oxide surface. The overall strategy allows us to isolate the catalytic effect of each individual parameter involved in a supported gold nanoparticle catalyst. We have successfully applied this methodology to develop green, efficient gold catalysts, such as the selective oxidation of ethanol by oxygen.

Supported gold nanoparticles are traditionally synthesized from single-atom gold precursors using aqueous chemistry. In the two most popular preparation methods (i.e., coprecipitation and deposition−precipitation), single-atom gold precursors are either coprecipitated with oxide precursors or directly deposited on an oxide surface. The size and size-distribution of gold nanoparticles formed during the calcination process, and the degree of dispersion on the support, are highly dependent on the following conditions: (1) pH and concentration of the precursor solution; (2) isoelectric point and type of the oxide support; (3) calcination temperature and procedure.[5] For example, the deposition−precipitation method (DP) requires the adjustment of pH value within the range of 6∼10 and is not applicable to acidic and hydrophobic supports such as SiO_2, WO_3, $SiO_2-Al_2O_3$, and activated carbon. A major challenge of conventional preparations is the difficulty of controlling the average size of gold nanoparticles and their size distribution on different oxide supports. The gold nanoparticles in the oxide-supported gold catalysts prepared by Haruta and co-workers typically have a particle-size standard deviation above 30%. Furthermore, although different loadings of gold nanoparticles can be achieved by changing the molar ratio of gold precursor to oxide support, they invariably do not have the same-sized gold nanoparticles.[9]

In contrast to aqueous-solution synthesis, Goodman and co-workers have successfully created model supported gold nanoparticle catalysts in high vacuum chambers for better fundamental understanding of the origin of their catalytic activity.[10] In both types of catalysts, however, the formation of gold nanoparticles is heavily influenced by the oxide supports because of the in situ formation of nanoparticles.[5,10] In comparison, the more controllable formation of isolated gold nanoparticles has been extensively studied through different wet-chemistry approaches during the past two decades.[11−13] The large-scale synthesis of nearly monodisperse gold nanoparticles with size standard deviation less than 10% has been recently achieved.[14−19] However, the lack of a general strategy to homogeneously disperse these gold nanoparticles on supports has limited their applications in catalysis.[7,20−25]

Prior to this work, presynthesized gold colloidal particles have been occasionally applied as precursors for the preparation of oxide-supported gold catalysts.[7,21−24] The presynthesized nanoparticles, which have a broad particle-size distribution, are generally deposited on oxide supports through mechanical mixing followed by evaporation.[21,22] As a result, the gold nanoparticles are not homogeneously dispersed on the oxide surface. These gold nanoparticles are frequently observed to sinter after thermal treatment to remove the organic ligands. The prepared catalysts do not show advantages in terms of controlling size or dispersion of nanoparticles.

In order to overcome the size-control problem, nearly monodisperse gold nanoparticles were synthesized using the single-phase, one-step synthesis that we recently developed.[16] The narrow size-distribution of gold nanoparticles is readily generated by using weak reducing agents (amine−borane complexes) rather than strong reductants (e.g., $NaBH_4$, $LiBH_4$) typically used. By selecting different reaction solvents and controlling the reaction temperatures, three different-sized monodisperse gold nanoparticles (i.e., 3.5 ± 0.5, 6.3 ± 0.5, and 8.2 ± 0.9 nm) were synthesized (Figure S1). The stable monodisperse gold nanoparticles were capped by long-chain alkyl thiols (e.g., dodecanethiol) and soluble in organic solvents (e.g., chloroform, dichloromethane, toluene, hexanes). The synthesized gold nanoparticles are hydrophobic owing to capping with long-chain alkyl thiols. The homogeneous dispersion of these hydrophobic nanoparticles on hydrophilic oxides can therefore be a problem.

Fortunately, we have found a route to circumvent this dispersion problem. The approach is based on the general concept of utilizing relatively weak interactions between metal nanoparticles and the substrates in an aprotic solvent to create a homogeneous loading of the nanoparticles. The dispersion is then locked in place by calcination. For the usual aqueous preparation procedures, columbic charge determined by the isoelectric points of the supporting oxides dominates the interaction with the metal nanoparticle precursors. In an aprotic solvent environment, oxide surfaces have a common feature, namely abundant permanent dipoles on their surface, which means that they preferably adsorb charged, polar, and highly

10.1021/ja0659929 CCC: $33.50 © 2006 American Chemical Society

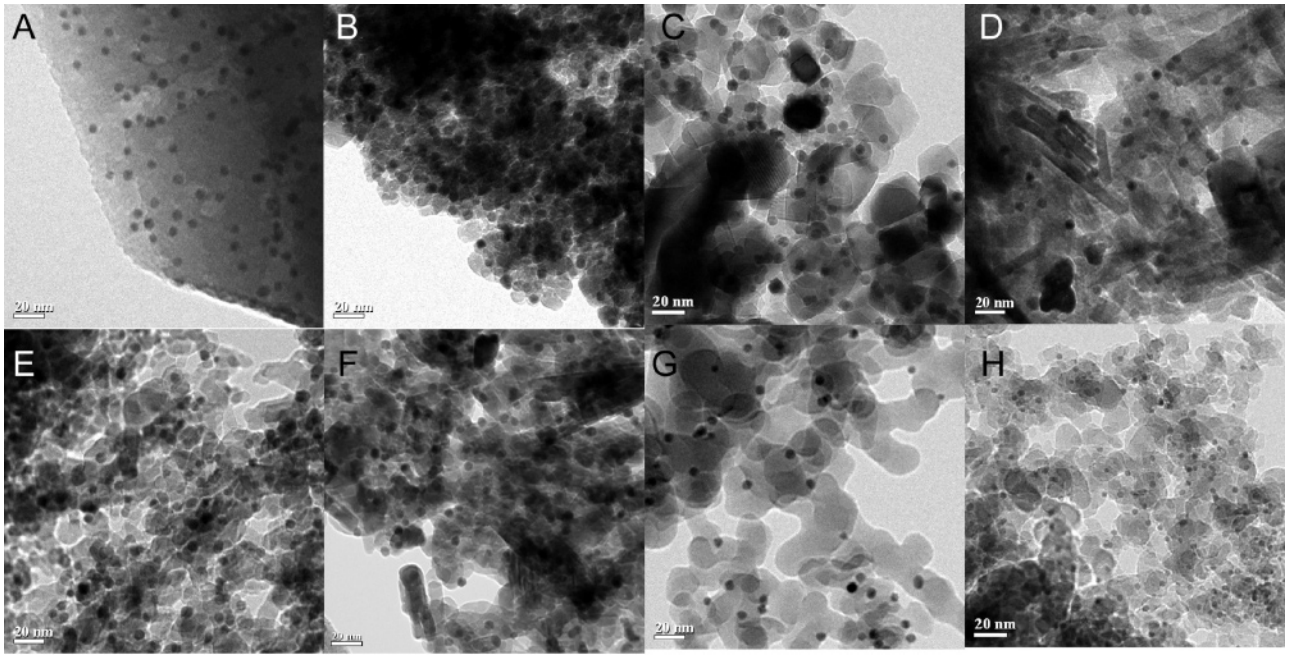

Figure 1. TEM images of 6.3 nm (A−G) and 3.5 nm (H) gold nanoparticles (5% in weight) supported on different oxides: (A) zeolite (CBV600); (B) α-Fe_2O_3; (C) TiO_2 (P25); (D) hydroxyapatite; (E) Al_2O_3; (F) ZnO; (G) fumed SiO_2; (H) SiO_2. The images were taken from the samples after thermal treatment at 300 °C in air for 1 h. All scale bars are 20 nm.

polarizable species, such as metal nanoparticles, through dipole−charge, dipole−dipole, and dipole−induced dipole interactions, respectively. When oxide powders (e.g., TiO_2, SiO_2, ZnO, Al_2O_3) are added to a solution of dodecanethiol-capped gold nanoparticles in an aprotic solvent (e.g., chloroform, methylenechloride), the gold solution is decolored while the color of the oxide powders darkens with stirring time (Figure S2). This adsorption behavior confirms the interaction between the hydrophobic gold nanoparticles and the hydrophilic oxides. We found that this interaction is rather weak and not competitive with conventional hydrogen bonding. The addition of a protic solvent (e.g., ethanol) can easily release the adsorbed gold nanoparticles from the oxide surface into the solution as evidenced by increased darkening of the liquid phase. This weak interaction between the gold nanoparticle and the metal oxide was observed for both charged and neutral organic-capped gold nanoparticles whose charge was characterized by electrophoretic mobility measurements (Figure S3). Therefore, the weak interaction between oxide particles and hydrophobic metal nanoparticles most likely is due to dipole−induced dipole or dipole−charge interactions.

By utilizing the weak interaction between metal-oxide particles and metal nanoparticles, as illustrated in Figure 1, we have successfully deposited gold nanoparticles on different supports ranging from very acidic oxides (e.g., zeolite in its acid form) to very basic oxides (e.g., ZnO) and from insulators (e.g., SiO_2) to semiconductors (e.g., TiO_2). The adsorption and desorption of metal nanoparticles kinetically occurs on the oxide surface when a solvent is present, which allows metal particles to migrate on the oxide surface during stirring. Therefore, it is not surprising that this kinetic process leads to the homogeneous dispersion of metal nanoparticles on oxide particles in all the metal-oxide composites we prepared. Another benefit of our general strategy is that same-sized metal nanoparticles can be easily loaded on supports in varying amounts by simply changing the amount of the oxide materials added into the metal nanoparticle solutions (Figure S4), which is technically difficult by conventional preparation methods. In addition to the deposition of gold nanoparticles, this assembly approach is also valid for the deposition of other metal nanoparticles (e.g., silver, gold-silver, platinum, palladium) on different oxides.

As noted above, the metal nanoparticles in the as-prepared metal-oxide composites are capped by organic thiols and do not possess catalytic properties. The capping ligands are removed by heating the prepared metal nanoparticle-oxide composites, typically in air at 300 °C for 1 h. After calcination, the ligands are decomposed and no sulfur is detected by XPS analysis. As illustrated in Figure 1, for both basic and acidic metal oxide supports, no obvious aggregation of gold nanoparticles is observed by TEM even though the gold nanoparticles in the calcined samples tend to wet the oxide surface during calcination. After the removal of the organic capping ligands, the gold nanoparticles are strongly bound to oxide supports and cannot be removed by protic organic solvents (e.g., methanol, ethanol). The supported gold nanoparticles even survive under acidic conditions (e.g., in 1 M HCl) when they are supported on nonbasic oxides (e.g., SiO_2, TiO_2).

In summary, in the synthetic strategy described here, both weak and strong interactions between metal-nanoparticles and oxides are involved in the different steps of the preparation, which, we believe, is crucial in order to obtain supported metal catalysts with well-defined physical and chemical properties. The weak interaction between hydrophobic metal nanoparticles and oxide nanoparticles, which we exploit for their cooperative assembly, allows controllable manipulations over both metal nanoparticles and oxide components of the catalysts since they are presynthesized individually. We believe that this assembly approach can help to bring together the well-developed nanomaterials synthesis with catalysis and sensing applications. Furthermore, the preparation of catalysts through cooperative assembly is also desirable to create multifunctional catalysts. For example, more than two types of metal nanoparticles can be simultaneously deposited on the same oxide. While the assembly step allows more control over individual components of the catalysts, the calcination step activates and stabilizes the metal nanoparticles. The collective benefit of this approach is desirable for the design of supported metal nanoparticle catalysts.

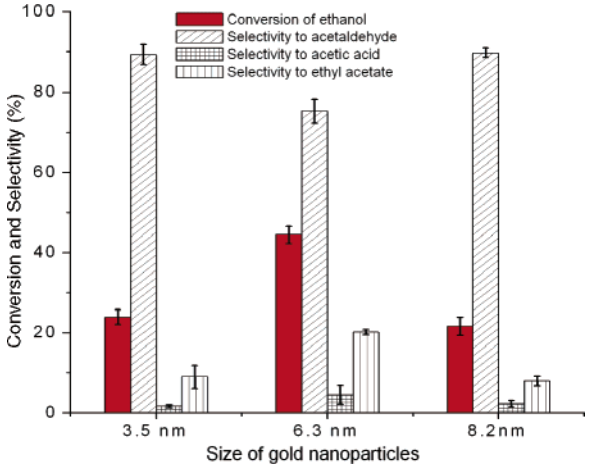

Figure 2. The size-dependent catalysis of ethanol oxidation by O_2 at 200 °C. Three catalysts with 3.5, 6.3, and 8.2 nm gold nanoparticles supported on SiO_2 (0.5% in weight) were used. Catalysis conditions: 1.000 g catalyst (0.5% Au on SiO_2), ethanol @ 0.6 mL/hour, and O_2 @10 mL/min.

To examine the catalytic properties of the supported gold nanoparticles prepared by the general strategy described above, we have chosen the selective oxidation of ethanol by oxygen. In order to study the size-dependent catalysis, three SiO_2-supported catalysts with 3.5, 6.3, and 8.2 nm gold nanoparticles were prepared by depositing the nanoparticles on chromatography silica gel in 0.5% (in weight) from their corresponding chloroform solution followed by calcination in air at 300 °C for 1 h. The catalytic properties of these three catalysts at 200 °C are shown in Figure 2. The smallest gold nanoparticles (3.5 nm) do not exhibit the high catalytic activity observed from 6.3 nm gold nanoparticles (conversion of 45% of ethanol). Both 3.5 and 8.2 nm nanoparticles have lower ethanol conversion (24% and 22%, respectively) but much higher selectivity to acetaldehyde (90%) than do the 6.3 nm particles (75%). While 6.3 nm Au nanoparticles give TOF (turn-over frequency to acetaldehyde) of 113 h^{-1}, TOFs are 80 and 73 h^{-1} for 3.5 and 8.2 nm particles, respectively.

After noting that 6.3 nm gold nanoparticles have a higher activity, we used them for ethanol oxidation under even milder conditions and found that SiO_2-supported 6.3 nm Au nanoparticles (2.5% of Au in weight) exhibit prominent catalysis with 21% ethanol conversion at 100 °C. The selectivity to ethyl acetate and acetaldehyde is 86% and 14%, respectively. When the gold loading is increased to 5%, the ethanol conversion reaches 39% with 90% selectivity to ethyl acetate. This catalytic production of ethyl acetate directly from ethanol by SiO_2-supported gold nanoparticles is unusual in its mild conditions used and the high selectivity that is realized. The only byproduct is acetaldehyde, which can also be used as a feedstock for ethyl acetate. The selective oxidation of alcohols catalyzed by SiO_2-supported gold nanoparticles prepared by other methods requires much harsher conditions, which might be due to their larger size.[26] It should also be noted that both copper- and palladium-based catalysts for the transformation of ethanol to ethyl acetate are also operated at temperatures higher than 200 °C and generate diverse byproducts.[27,28]

Acknowledgment. This work was supported by the NASA University Research Engineering and Technology Institute on Bio Inspired Materials (BiMat) under Award No. NCC-1-02037 and made use of the MRL central facilities supported by the MRSEC Program of the National Science Foundation under Award No. DMR05-20415. We thank Prof. Horia Metiu and Prof. Jacob Israelachvili for helpful discussions and Dr. Peter Stoimenov for XPS measurement. We also thank Degussa for providing oxide samples.

Supporting Information Available: Materials used for this study, synthesis and catalysis of oxide-supported metal nanoparticles, the decoloring of gold nanoparticles upon the addition of oxide powders, electrophoretic mobility measurements, gold nanoparticle size-distribution, and XPS spectra before and after calcination. This material is available free of charge via the Internet at http://pubs.acs.org.

References

(1) (a) Choudhary, T. V.; Goodman, D. W. *Top. Catal.* **2002**, *21*, 25−34. (b) Choudhary, T. V.; Goodman, D. W. *App. Catal., A* **2005**, *32*, *32*−36.
(2) (a) Bond, G. C.; Thompson, D. T. *Catal. Rev.-Sci. Eng.* **1999**, 41, 319−388. (b) Bond, G. C.; Thompson, D. T. *Appl. Catal., A* **2006**, *302*, 1−4.
(3) (a) Hutchings, G. J. *Catal. Today* **2005**, *100*, 55−61. (b) Hutchings, G. J.; Haruta, M. *Appl. Catal., A* **2005**, *291*, 2−5. (c) Haruta, M. *Gold Bull.* **2004**, *37*, 27−36.
(4) Didier Astruc, F. L.; Aranzaes, J. R. *Angew. Chem., Int. Ed.* **2005**, *44*, 7852−7872 and references therein.
(5) (a) Haruta, M. *CATTECH* **2002**, *6*, 102−115. (b) Haruta, M. *Catal. Today* **1997**, *36*, 153−166.
(6) Campbell, C. T. *Science* **2004**, *306*, 234−235.
(7) Comotti, M.; Li, W. C.; Spliethoff, B.; Schuth, F. *J. Am. Chem. Soc.* **2006**, *128*, 917−924.
(8) Schubert, M. M.; Hackenberg, S.; van Veen, A. C.; Muhler, M.; Plzak, V.; Behm, R. J. *J. Catal.* **2001**, *197*, 113−122.
(9) Bamwenda, G. R.; Tsubota, S.; Nakamura, T.; Haruta, M. *Catal. Lett.* **1997**, *44*, 83−87.
(10) (a) Chen, M. S.; Goodman, D. W. *Science* **2004**, *306*, 252−255. (b) Chen, M. S.; Goodman, D. W. *Catal. Today* **2006**, *111*, 22−33.
(11) Daniel, M. C.; Astruc, D. *Chem. Rev.* **2004**, *104*, 293−346 and references therein.
(12) Brust, M.; Walker, M.; Bethell, D.; Schiffrin, D. J.; Whyman, R. *Chem. Commun.* **1994**, 801−802.
(13) Schmid, G. *Nanoparticles: From Theory to Application;* Wiley-VCH: Weinheim, Germany, 2004 and references therein.
(14) (a) Stoeva, S. I.; Prasad, B. L. V.; Uma, S.; Stoimenov, P. K.; Zaikovski, V.; Sorensen, C. M.; Klabunde, K. J. t. *J. Phys. Chem. B* **2003**, *107*, 7441−7448. (b) Stoeva, S.; Klabunde, K. J.; Sorensen, C. M.; Dragieva, I. *J. Am. Chem. Soc.* **2002**, *124*, 2305−2311. (c) Prasad, B. L. V.; Stoeva, S. I.; Sorensen, C. M.; Klabunde, K. J. *Langmuir* **2002**, *18*, 7515−7520.
(15) Jana, N. R.; Peng, X. G. *J. Am. Chem. Soc.* **2003**, *125*, 14280−14281.
(16) Zheng, N.; Fan, J.; Stucky, G. D. *J. Am. Chem. Soc.* **2006**, *128*, 6550−6551.
(17) Tsunoyama, H.; Negishi, Y.; Tsukuda, T. *J. Am. Chem. Soc.* **2006**, *128*, 6036−6037.
(18) Templeton, A. C.; Wuelfing, M. P.; Murray, R. W. *Acc. Chem. Res.* **2000**, *33*, 27−36.
(19) Schaaff, T. G.; Whetten, R. L. *J Phys. Chem. B* **2000**, *104*, 2630−2641.
(20) Maye, M. M.; Luo, J.; Han, L.; Kariuki, N. N.; Zhong, C. J. *Gold Bull.* **2003**, *36*, 75−82.
(21) Chou, J.; McFarland, E. W. *Chem. Commun.* **2004**, 1648−1649.
(22) Tsubota, S.; Nakamura, T.; Tanaka, K.; Haruta, M. *Catal. Lett.* **1998**, *56*, 131−135.
(23) Grunwaldt, J. D.; Kiener, C.; Wogerbauer, C.; Baiker, A. *J. Catal.* **1999**, *181*, 223−232.
(24) Pietron, J. J.; Stroud, R. M.; Rolison, D. R. *Nano Lett.* **2002**, *2*, 545−549.
(25) Tai, Y.; Murakami, J.; Tajiri, K.; Ohashi, F.; Date, M.; Tsubota, S. *Appl. Catal., A* **2004**, *268*, 183−187.
(26) (a) Biella, S.; Rossi, M. *Chem. Commun.* **2003**, 378−379. (b) Ma, Y; Shi, F; Deng, Y. *J. Mol. Catal. (China)* **2003**, *17*, 425−429.
(27) Fawcett, C. R.; Tuck, M. W. M.; Watson, D. J.; Sharif, C. M.; Colley, S. W.; Wood, M. A. Patent WO 0020373, 2000.
(28) Sanchez, A. B.; Homs, N.; Fierro, J. L. G.; de la Piscina, P. R. *Catal. Today* **2005**, *107*−*108*, 431−435.

JA0659929